such as spike-count correlations (*23*), can be understood as arising from the On-Off dynamics (fig. S12 and supplementary text 3.8). Correlated variability can be affected by cognitive factors (*24*–*26*). In particular, spike-count correlations can increase or decrease during selective attention (*27*–*30*), and changes in the On-Off dynamics account for changes in spike-count correlations during attention in our data (fig. S13 and supplementary text 3.8.4). Recent models parsimoniously attribute changes in spike-count correlations during attention to fluctuations in shared modulatory signals (*31*), with smaller spike-count correlations accounted for by reduced fluctuations in these modulatory signals (*32*). The On-Off dynamics observed here could underlie the apparent trial-to-trial fluctuations in shared modulatory signals (*32*, *33*) but can account for within-trial fluctuations as well (fig. S12 and supplementary text 3.8.5).

What mechanisms underlie the spatially and temporally precise control of cortical state during selective attention? Our results suggest that global mechanisms governing cortical states may themselves also operate on a local scale or, alternatively, may interact with separate attentional control mechanisms operating locally. Indeed, neuromodulators known to act on a brain-wide scale (*1*, *34*, *35*) also mediate the effects of selective attention (*36*) and influence circuits that control selective attention (*37*). On the other hand, cortico-cortical inputs appear to influence state changes in a spatially targeted manner (*38*, *39*). Because diffuse neuromodulatory signals are interspersed with topographically precise projections throughout the cortex, local modulation of cortical state is likely to be widespread, extending to modalities beyond vision and serving many cognitive functions.

REFERENCES AND NOTES

1. K. D. Harris, A. Thiele, *Nat. Rev. Neurosci.* **12**, 509–523 (2011).
2. S.-H. Lee, Y. Dan, *Neuron* **76**, 209–222 (2012).
3. M. Steriade, D. A. McCormick, T. J. Sejnowski, *Science* **262**, 679–685 (1993).
4. M. Steriade, I. Timofeev, F. Grenier, *J. Neurophysiol.* **85**, 1969–1985 (2001).
5. B. Haider, A. Duque, A. R. Hasenstaub, Y. Yu, D. A. McCormick, *J. Neurophysiol.* **97**, 4186–4202 (2007).
6. A. Hasenstaub, R. N. S. Sachdev, D. A. McCormick, *J. Neurosci.* **27**, 9607–9622 (2007).
7. A. Renart *et al.*, *Science* **327**, 587–590 (2010).
8. S. Crochet, C. C. H. Petersen, *Nat. Neurosci.* **9**, 608–610 (2006).
9. J. F. A. Poulet, C. C. H. Petersen, *Nature* **454**, 881–885 (2008).
10. C. M. Niell, M. P. Stryker, *Neuron* **65**, 472–479 (2010).
11. M. Okun, A. Naim, I. Lampl, *J. Neurosci.* **30**, 4440–4448 (2010).
12. A. Luczak, P. Bartho, K. D. Harris, *J. Neurosci.* **33**, 1684–1695 (2013).
13. A. Y. Y. Tan, Y. Chen, B. Scholl, E. Seidemann, N. J. Priebe, *Nature* **509**, 226–229 (2014).
14. N. A. Steinmetz, T. Moore, *Neuron* **83**, 496–506 (2014).
15. E. Seidemann, I. Meilijson, M. Abeles, H. Bergman, E. Vaadia, *J. Neurosci.* **16**, 752–768 (1996).
16. G. Rainer, E. K. Miller, *Neurocomputing* **32-33**, 961–966 (2000).
17. M. Vinck, R. Batista-Brito, U. Knoblich, J. A. Cardin, *Neuron* **86**, 740–754 (2015).
18. J. Reimer *et al.*, *Neuron* **84**, 355–362 (2014).
19. J. Moran, R. Desimone, *Science* **229**, 782–784 (1985).
20. S. Treue, J. H. Maunsell, *Nature* **382**, 539–541 (1996).
21. P. Fries, J. H. Reynolds, A. E. Rorie, R. Desimone, *Science* **291**, 1560–1563 (2001).
22. A. Renart, C. K. Machens, *Curr. Opin. Neurobiol.* **25**, 211–220 (2014).
23. M. R. Cohen, A. Kohn, *Nat. Neurosci.* **14**, 811–819 (2011).
24. M. R. Cohen, W. T. Newsome, *Neuron* **60**, 162–173 (2008).
25. Y. Gu *et al.*, *Neuron* **71**, 750–761 (2011).
26. A. S. Ecker *et al.*, *Neuron* **82**, 235–248 (2014).
27. J. F. Mitchell, K. A. Sundberg, J. H. Reynolds, *Neuron* **63**, 879–888 (2009).
28. M. R. Cohen, J. H. R. Maunsell, *Nat. Neurosci.* **12**, 1594–1600 (2009).
29. D. A. Ruff, M. R. Cohen, *Nat. Neurosci.* **17**, 1591–1597 (2014).
30. D. A. Ruff, M. R. Cohen, *J. Neurosci.* **36**, 7523–7534 (2016).
31. R. L. T. Goris, J. A. Movshon, E. P. Simoncelli, *Nat. Neurosci.* **17**, 858–865 (2014).
32. N. C. Rabinowitz, R. L. Goris, M. Cohen, E. P. Simoncelli, *eLife* **4**, e08998 (2015).
33. M. R. Cohen, J. H. R. Maunsell, *J. Neurosci.* **30**, 15241–15253 (2010).
34. G. Aston-Jones, J. D. Cohen, *Annu. Rev. Neurosci.* **28**, 403–450 (2005).
35. T. W. Robbins, A. F. T. Arnsten, *Annu. Rev. Neurosci.* **32**, 267–287 (2009).
36. J. L. Herrero *et al.*, *Nature* **454**, 1110–1114 (2008).
37. B. Noudoost, T. Moore, *Nature* **474**, 372–375 (2011).
38. E. Zagha, A. E. Casale, R. N. S. Sachdev, M. J. McGinley, D. A. McCormick, *Neuron* **79**, 567–578 (2013).
39. G. G. Gregoriou, S. J. Gotts, H. Zhou, R. Desimone, *Science* **324**, 1207–1210 (2009).

ACKNOWLEDGMENTS

This work was supported by NIH grants EY014924 and NS076460, a Stanford NeuroVentures grant, Medical Research Council (MRC) grant MR/K013785/1, and Wellcome Trust grant 093104. We thank E. I. Knudsen, K. Harris, S. Ganguli, R. N. S. Sachdev, and M. Zirnsak for their comments on the manuscript. We thank D. S. Aldrich for technical assistance. All behavioral and electrophysiological data are presented in (*14*) and are archived at the Stanford Neuroscience Institute server at Stanford University. T.A.E., N.A.S., T.M., and K.B. designed the study. N.A.S. and T.M. designed the experiments. N.A.S. performed experiments, spike sorting, microsaccade detection, and RF measurements. M.A.G. and A.T. performed experiments for the additional laminar data set. T.A.E. analyzed and modeled the data. T.A.E., N.A.S., T.M., and K.B. discussed the findings and wrote the paper.

SUPPLEMENTARY MATERIALS

www.sciencemag.org/content/354/6316/1140/suppl/DC1
Materials and Methods
Supplementary Text
Figs. S1 to S13
Table S1
References (*40*–*58*)

16 May 2016; accepted 31 October 2016
10.1126/science.aag1420

PAIN RESEARCH

Gliogenic LTP spreads widely in nociceptive pathways

M. T. Kronschläger,* R. Drdla-Schutting,* M. Gassner, S. D. Honsek, H. L. Teuchmann, J. Sandkühler†

Learning and memory formation involve long-term potentiation (LTP) of synaptic strength. A fundamental feature of LTP induction in the brain is the need for coincident pre- and postsynaptic activity. This restricts LTP expression to activated synapses only (homosynaptic LTP) and leads to its input specificity. In the spinal cord, we discovered a fundamentally different form of LTP that is induced by glial cell activation and mediated by diffusible, extracellular messengers, including D-serine and tumor necrosis factor (TNF), and that travel long distances via the cerebrospinal fluid, thereby affecting susceptible synapses at remote sites. The properties of this gliogenic LTP resolve unexplained findings of memory traces in nociceptive pathways and may underlie forms of widespread pain hypersensitivity.

Activity-dependent, homosynaptic long-term potentiation (LTP) (*1*) at synapses in nociceptive pathways contributes to pain amplification (hyperalgesia) at the site of an injury or inflammation (*2*–*5*). Homosynaptic LTP can, however, not account for pain amplification at areas surrounding (secondary hyperalgesia) or remote from (widespread hyperalgesia) an injury. It also fails to explain hyperalgesia that is induced independently of neuronal activity in primary afferents—e.g., by the application of or the withdrawal from opioids (opioid-induced hyperalgesia) (*6*). Glial cells are believed to contribute to these forms of hyperalgesia and to LTP in nociceptive pathways (*7*–*10*). Induction of homosynaptic LTP can be accompanied by LTP in adjacent, inactive synapses converging onto the same neuron, especially early in development. The respective molecular signals for this heterosynaptic form of LTP are thought to be confined within the cytoplasm of the activated neuron, spreading tens of micrometers only (*11*). We have now tested the hypothesis that, in contrast to current beliefs, activation of glial cells is causative for the induction of LTP at spinal C-fiber synapses and that this gliogenic LTP constitutes a common denominator of homo- and heterosynaptic LTP in the spinal cord.

Our previous study revealed that selective activation of spinal microglia by fractalkine induces

Department of Neurophysiology, Center for Brain Research, Medical University of Vienna, Spitalgasse 4, 1090 Vienna, Austria.
*These authors contributed equally to this work. **†Corresponding author. Email: juergen.sandkuehler@meduniwien.ac.at**

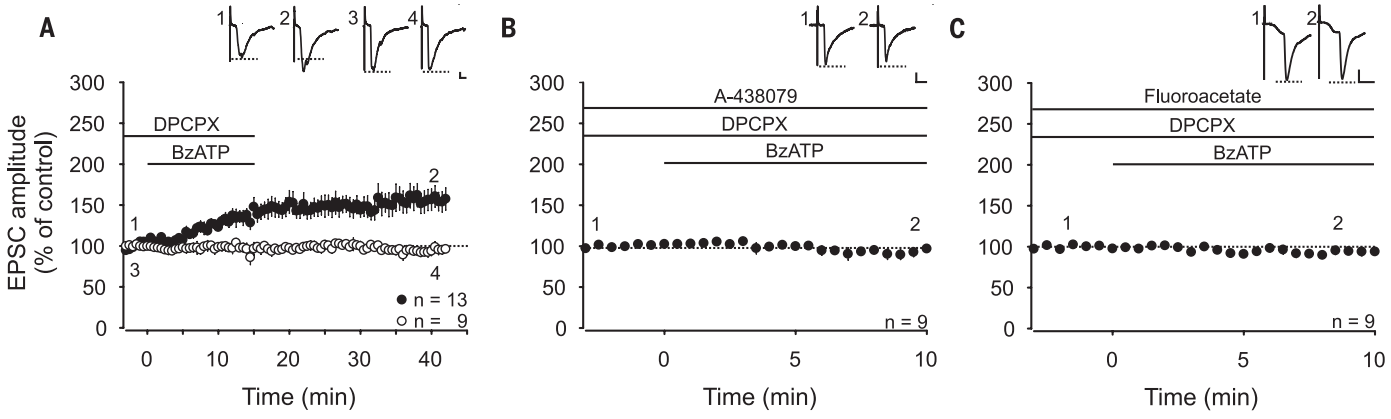

Fig. 1. Activation of spinal P2X$_7$ receptors induces gliogenic LTP at C-fiber synapses. Recordings were performed on lamina I neurons with independent monosynaptic C-fiber inputs from two dorsal root halves. Amplitudes of EPSCs were normalized to six baseline values, and the mean (±1 SEM) was plotted against time (min). Horizontal bars indicate drug application. (**A**) DPCPX (1 μM) application started at time point −3 min. Bath application of BzATP (100 μM) started at time point 0 min and induced LTP at 13 out of 22 C-fiber inputs (filled circles) ($P < 0.001$, at 30 min of wash-out compared with control values). At 9 out of 22 C-fiber inputs, BzATP did not influence EPSC amplitudes (open circles) ($P = 0.650$, at 30 min of wash-out compared with control values). (**B**) Bath application of the P2X$_7$R antagonist A-438079 (10 μM) 13 min before BzATP prevented the BzATP-induced LTP at all C-fiber inputs tested ($n = 9$, $P = 0.054$, at 10 min compared with baseline). (**C**) In the presence of fluoroacetate (10 μM), BzATP had no effect on synaptic transmission ($n = 9$, $P = 0.114$ at 10 min compared to baseline). Insets show individual EPSCs at indicated time points. Calibration bars indicate 50 pA and 10 ms. Statistical significance was determined by using repeated measures analysis of variance (RM ANOVA) followed by Bonferroni *t* test. Paired *t* test was used for control recordings.

transient facilitation, but no LTP, at C-fiber synapses (*12*). Here, we recorded monosynaptic C-fiber–evoked excitatory postsynaptic currents (EPSCs) from lamina I neurons in rat lumbar spinal cord slices. To investigate whether selective activation of spinal astrocytes is sufficient for the induction of synaptic plasticity in the absence of any other conditioning stimulus, we used ultraviolet (UV)–flash photolysis of caged inositol 1,4,5-trisphosphate (IP$_3$) in astrocytic networks (fig. S1 and movie S1). This induced a robust long-term depression at C-fiber synapses (gliogenic LTD; to 69 ± 9%, $n = 7$, $P < 0.001$) (fig. S1C) but no LTP. UV flashes were without any effect on synaptic strength when applied in the absence of caged IP$_3$ (fig. S1D) or in the presence of the glial cell toxin fluoroacetate (fig. S1E). To coactivate microglia and astrocytes, we next applied the purinergic P2X$_7$ receptor (P2X$_7$R) agonist benzoyl-benzoyl adenosine triphosphate (BzATP). This never affected holding currents or membrane potentials in any of the spinal neurons tested (fig. S2), supporting the observation that, in the spinal dorsal horn, and unlike other P2X receptors (*13*), P2X$_7$Rs are expressed exclusively on glial cells (*14*–*18*). ATP is finally hydrolyzed to adenosine. We therefore applied the adenosine 1 receptor antagonist DPCPX to block adenosine-mediated presynaptic inhibition (fig. S3). Combined activation of microglia and astrocytes by BzATP induced LTP in 13 out of 22 C-fiber inputs (to 156 ± 13%, $P < 0.001$) (Fig. 1A). BzATP-induced LTP was abolished by the selective P2X$_7$R antagonist A-438079 (Fig. 1B) and by fluoroacetate (Fig. 1C). This demonstrates that selective activation of P2X$_7$R on spinal glial cells caused gliogenic LTP at synapses between C fibers and lamina I neurons.

High-frequency stimulation (HFS) of primary afferent C fibers triggers the release of ATP from primary afferent neurons (*19*, *20*), activates glial cells (*21*, *22*), and induces LTP (*2*, *3*), leading to the intriguing hypothesis that HFS-induced LTP at spinal C-fiber synapses might be a variety of gliogenic LTP. If true, one would predict that HFS induces LTP not only at conditioned but also at unconditioned C-fiber synapses and that, in striking contrast to current beliefs, homo- and heterosynaptic LTP could be expressed independently of each other. To directly test these predictions, we used transverse lumbar spinal cord slices with long dorsal roots attached that were separated into halves. We recorded from 22 dorsal horn lamina I neurons that received independent monosynaptic C-fiber input from each dorsal root half. HFS applied to one dorsal root half induced LTP in the conditioned pathway in 12 of these neurons ("homosynaptic LTP"; to 134 ± 9%, $P < 0.001$) (Fig. 2Aa, red filled circles). Out of these 12 neurons, where homosynaptic LTP was induced, 6 also showed LTP at the unconditioned pathway ("heterosynaptic LTP"). In total, heterosynaptic LTP was induced in 11 out of 22 neurons (to 174 ± 19%, $P < 0.001$) (Fig. 2Ba, blue filled circles) because, importantly, in 5 of these neurons, heterosynaptic LTP was induced in the absence of homosynaptic LTP (to 161 ± 9%, $P < 0.005$) (Fig. 2C), a finding that cannot be explained by current models of synaptic plasticity.

We investigated whether HFS-induced homo- and heterosynaptic LTP require activation of glial cells via P2X$_7$R. Blockade of glial P2X$_7$R by A-438079 fully blocked LTP induction at the conditioned and at the unconditioned sites (Fig. 2, Ab and Bb). This was also achieved by blocking glial cell metabolism with fluoroacetate [Fig. 2, Ac and Bc and (*21*)]. Both homo- and heterosynaptic LTP were abolished by blocking postsynaptic *N*-methyl-D-aspartate receptors (NMDARs) (Fig. 2, Ad and Bd). D-serine is a coagonist at NMDARs that is released from astrocytes (*23*). Here, preincubation of slices with the D-serine–degrading enzyme D-amino acid oxidase (DAAO) abolished both homo- and heterosynaptic LTP (Fig. 2, Ae and Be). We then investigated whether D-serine alone is sufficient to enhance synaptic strength at C-fiber synapses. Bath application of D-serine facilitated synaptic strength at C-fiber synapses (to 120 ± 2% in 13 out of 32 cells; $P < 0.001$) (fig. S4A). This amplification was abolished by blockade of NMDARs (in 12 out of 13 cells; $P = 0.094$) (fig. S4B). Taken together, our data demonstrate that the combined activation of microglia and astrocytes, either via P2X$_7$R or by HFS, was sufficient to induce gliogenic LTP. When gliogenic LTP is induced by conditioning HFS, it may appear as homo- and/or heterosynaptic LTP that can be elicited independently of each other.

We next asked whether gliogenic LTP also exists in vivo. HFS applied to the sciatic nerve induced LTP of spinal C-fiber–evoked field potentials in deeply anesthetized rats (to 211 ± 16% at 220 to 240 min; $n = 49$, $P < 0.001$) (Fig. 3A). HFS-induced LTP was blocked by spinal application of either fluoroacetate (Fig. 3B) or DAAO (Fig. 3C), indicating that it required the activation of spinal glial cells and D-serine signaling. Application of fluoroacetate or DAAO after the induction of LTP had no effects on LTP maintenance (to 192 ± 23% and to 181 ± 30%, respectively, at 220 to 240 min; $n = 6$; $P = 0.433$ and 0.546, respectively) (fig. S5), indicating that once LTP was induced, glial cells were no longer required. Thus, the gliogenic nature refers to the induction but not to the maintenance phase of LTP.

We then investigated whether HFS leads to the release of diffusible mediators that spread over long distances to trigger LTP. We induced LTP by HFS, collected the spinal superfusate from the respective lumbar segments, and transferred

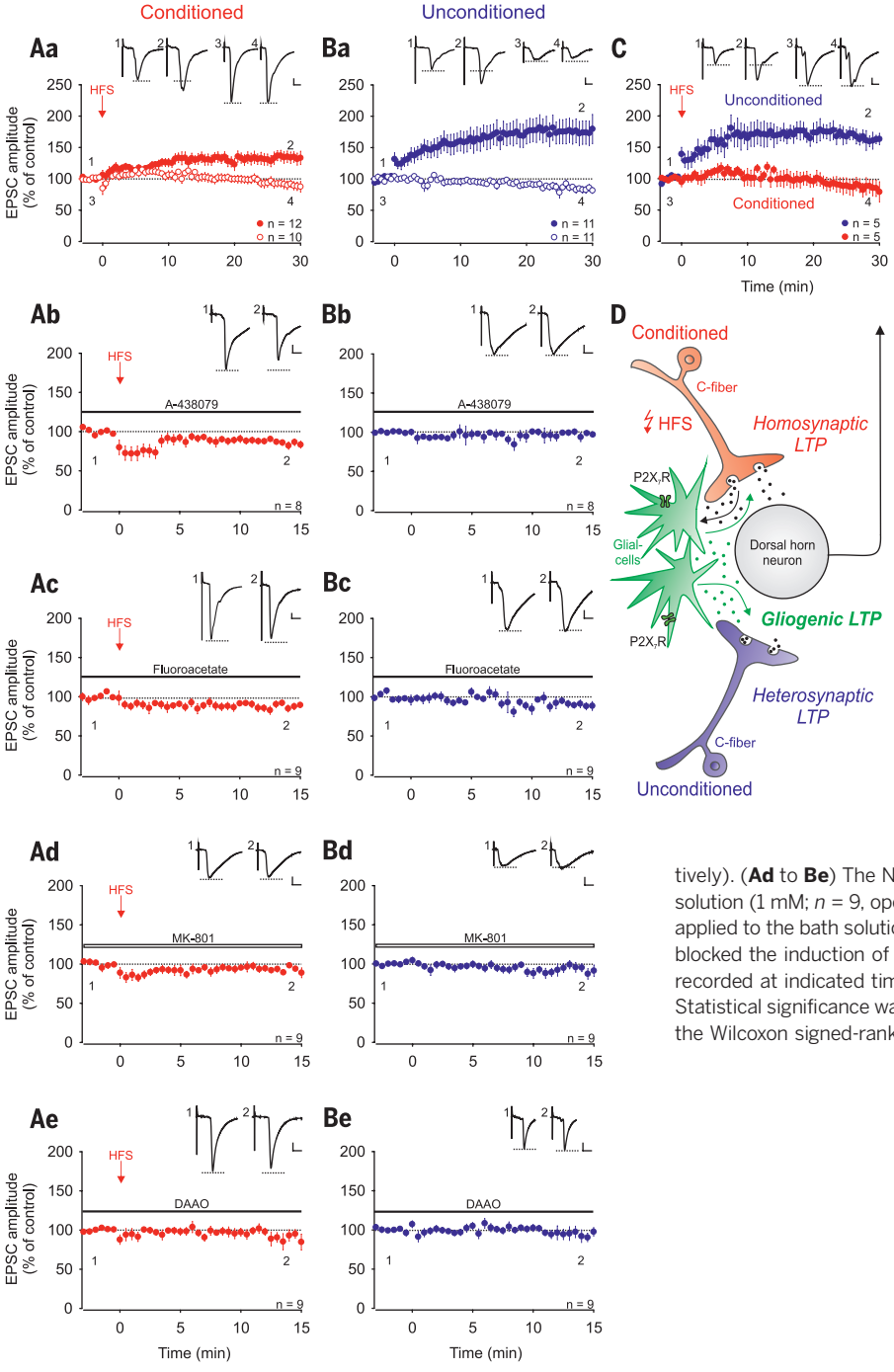

Fig. 2. Homo- and heterosynaptic forms of LTP are induced independently of each other at C-fiber synapses by conditioning HFS. Recordings were performed on lamina I neurons with independent monosynaptic C-fiber inputs from two dorsal root halves. Amplitudes of EPSCs were normalized to six baseline values and the mean (±1 SEM) was plotted against time (min). HFS was applied to one dorsal root (arrow; conditioned site in red) at time point 0 min. Horizontal bars indicate drug application. (**Aa**) HFS induced LTP at conditioned synapses in 12 out of 22 neurons (homosynaptic LTP in red, filled circles; $P < 0.001$, at 30 min compared with control values). In 10 of these neurons, no homosynaptic LTP was induced (open circles; $P = 0.105$). (**Ba**) HFS induced LTP at unconditioned synapses in 11 out of the same 22 neurons tested (heterosynaptic LTP in blue, filled circles; $P < 0.001$, at 30 min compared with control values). In 11 of these neurons, no heterosynaptic LTP was observed (open circles; $P = 0.003$). (**C**) In 5 out of these 22 neurons tested, HFS induced LTP at unconditioned (filled circles in blue; 161 ± 10%, $P = 0.005$) but not at conditioned synapses (filled circles in red; $P = 0.313$). (**D**) Schematic illustration of homo- and heterosynaptic forms of LTP as varieties of gliogenic LTP. (**Ab** and **Bb**) HFS failed to induce LTP at the conditioned site in the presence of A-438079 (10 μM; $n = 8$, $P = 0.006$). A-438079 had no effect on EPSC amplitudes at unconditioned synapses. (**Ac** and **Bc**) In the presence of fluoroacetate, LTP induction by HFS was abolished at conditioned and at unconditioned sites (10 μM; $n = 9$, $P = 0.006$ and $P = 0.034$, respectively). (**Ad** to **Be**) The NMDAR blocker MK-801, which was added to the pipette solution (1 mM; $n = 9$, open bar; $P = 0.044$ and $P = 0.250$, respectively) or DAAO applied to the bath solution (0.2 U·ml^{-1}; $n = 9$, $P = 0.006$ and 0.572, respectively) blocked the induction of LTP on both sites. Insets show individual EPSC traces recorded at indicated time points. Calibration bars indicate 100 pA and 10 ms. Statistical significance was determined by paired *t* test. In case of non-normality, the Wilcoxon signed-rank test was used.

it to the spinal cord dorsum of naïve animals. The maintenance of LTP in the donor animals was not affected by exchanging the superfusate (Fig. 3A). The superfusate induced, however, a robust LTP in the recipient animals (to 173 ± 32% of control at 160 to 180 min; $n = 10$, $P = 0.009$) (Fig. 4A), demonstrating that LTP could be transferred between individuals. The superfusate collected from naïve donor animals had, in contrast, no effect on synaptic transmission in any of the recipient animals (Fig. 4B). When glial cells were blocked in the recipient animals, "transferable LTP" was still induced (to 160 ± 20%; $n = 9$, $P < 0.001$) (Fig. 4C). Blockade of interleukin-1β (IL-1β) signaling in the recipient animals also had no effect on the induction of transferable LTP (to 133 ± 12% at 180 to 240 min; $n = 10$, $P = 0.001$) (Fig. 4D). However, LTP induction was prevented by blocking TNF (Fig. 4E), D-serine signaling (Fig. 4F), or spinal NMDARs (Fig. 4G) in the recipient animals. Application of D-serine to the spinal cord dose-dependently induced a reversible synaptic facilitation (to 152 ± 9% at 220 to 240 min; $n = 10$, $P < 0.001$) (fig. S6), whereas TNF application triggers robust LTP at C-fiber synapses (*21*). These data indicate that transferable LTP required activation of glial cells in the donor but not in the recipient animals and that the combined actions of the gliotransmitters D-serine and TNF were required for its induction.

Collectively, our data indicate that the combined activation of microglia and astrocytes, either by $P2X_7R$ agonists or by HFS of primary afferents, triggered gliogenic LTP at C-fiber synapses with spinal lamina I neurons through the release of D-serine and cytokines such as TNF. Crucially, glial cell–derived signaling molecules accumulated in the extracellular space, including the cerebrospinal fluid, at biologically active but presently unknown concentrations, and induced LTP at C-fiber synapses, constituting the phenomenon of gliogenic LTP.

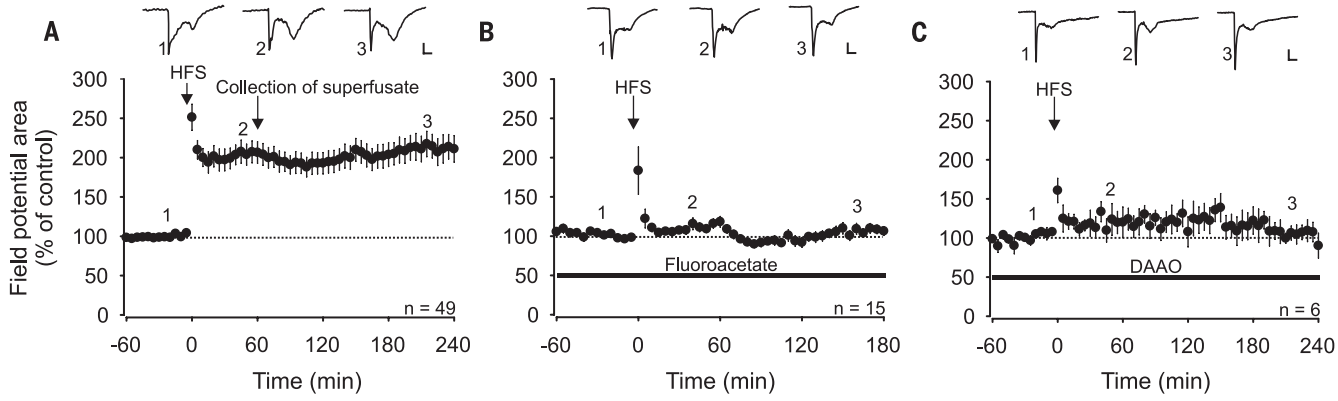

Fig. 3. HFS-induced LTP in vivo depends on spinal glial cells and D-serine signaling. Area of C-fiber–evoked field potentials was normalized to baseline values before conditioning HFS and plotted against time (min). Data are expressed as mean ± 1 SEM. Horizontal bars indicate drug application. (**A**) Mean time course of LTP of C-fiber–evoked field potentials. HFS at time point 0 min (arrow) induced LTP in all animals tested ($n = 49$, $P < 0.001$). One hour after HFS, the superfusate was collected from the lumbar spinal cord dorsum and transferred to animals shown in Fig. 4. (**B**) Spinal superfusion with the glial inhibitor fluoroacetate (10 μM) fully blocked HFS-induced potentiation in all animals tested ($n = 15$, $P = 0.085$). (**C**) HFS-induced LTP was fully prevented by spinal superfusion with DAAO (1 U·ml^{-1}; $n = 6$, $P = 0.365$). Insets show original traces of field potentials recorded at indicated time points. Calibration bars indicate 0.2 mV and 50 ms. RM ANOVA on ranks was performed to determine statistical significance in (A). In all other experiments, data were analyzed by using RM ANOVA.

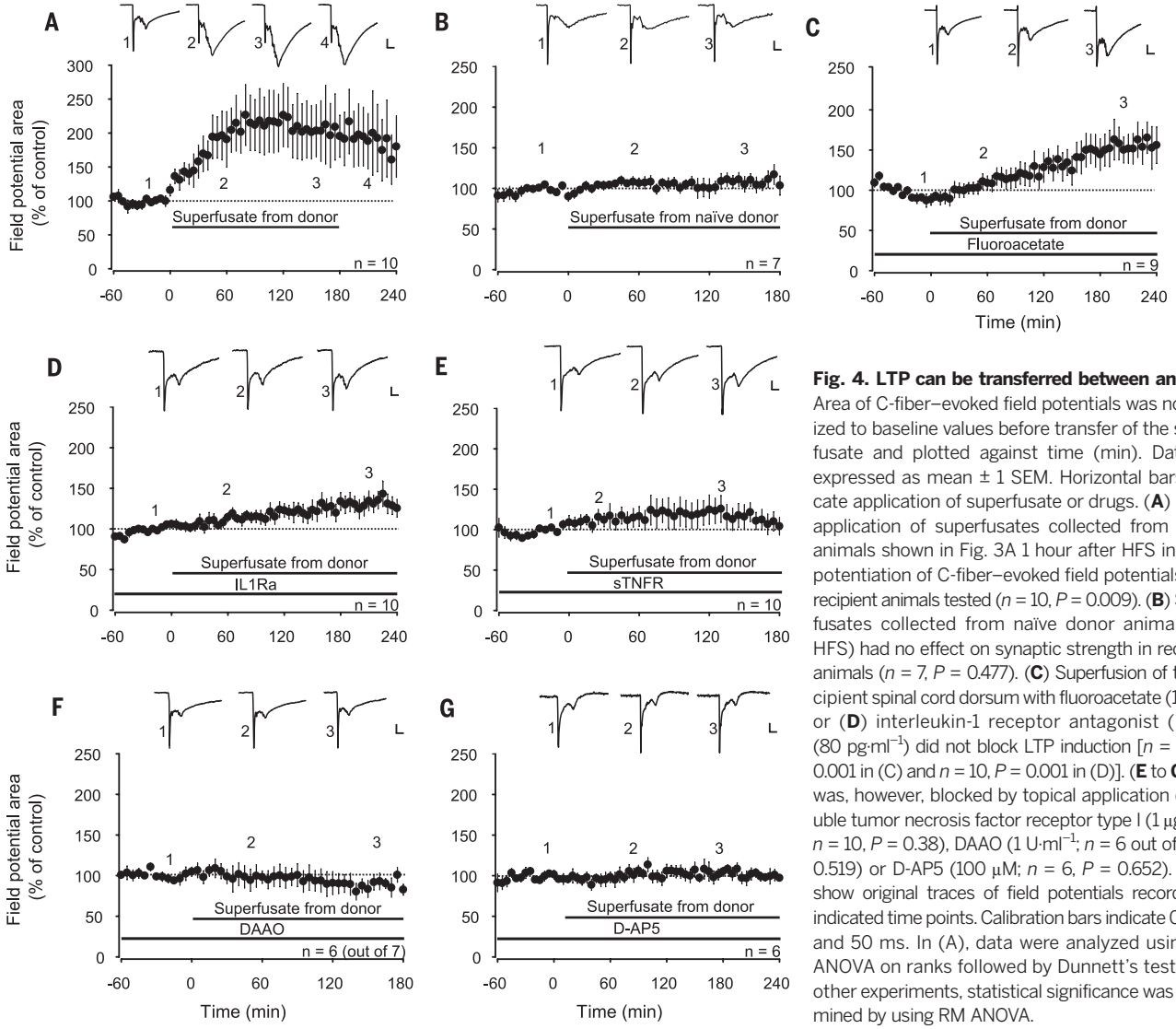

Fig. 4. LTP can be transferred between animals. Area of C-fiber–evoked field potentials was normalized to baseline values before transfer of the superfusate and plotted against time (min). Data are expressed as mean ± 1 SEM. Horizontal bars indicate application of superfusate or drugs. (**A**) Spinal application of superfusates collected from donor animals shown in Fig. 3A 1 hour after HFS induced potentiation of C-fiber–evoked field potentials in all recipient animals tested ($n = 10$, $P = 0.009$). (**B**) Superfusates collected from naïve donor animals (no HFS) had no effect on synaptic strength in recipient animals ($n = 7$, $P = 0.477$). (**C**) Superfusion of the recipient spinal cord dorsum with fluoroacetate (10 μM) or (**D**) interleukin-1 receptor antagonist (IL1Ra) (80 pg·ml^{-1}) did not block LTP induction [$n = 9$, $P < 0.001$ in (C) and $n = 10$, $P = 0.001$ in (D)]. (**E** to **G**) LTP was, however, blocked by topical application of soluble tumor necrosis factor receptor type I (1 μg·ml^{-1}; $n = 10$, $P = 0.38$), DAAO (1 U·ml^{-1}; $n = 6$ out of 7, $P = 0.519$) or D-AP5 (100 μM; $n = 6$, $P = 0.652$). Insets show original traces of field potentials recorded at indicated time points. Calibration bars indicate 0.2 mV and 50 ms. In (A), data were analyzed using RM ANOVA on ranks followed by Dunnett's test. In all other experiments, statistical significance was determined by using RM ANOVA.

Gliogenic LTP is a new form of paracrine synaptic plasticity in the central nervous system and may lead to pain amplification close to and remote from an injury or an inflammation. This is in line with the concept of chronic pain as a gliopathy involving neurogenic neuroinflammation (*7*, *24*). These new insights may pave the way for novel pain therapies (*25*, *26*). $P2X_7Rs$ play a key role in chronic inflammatory and neuropathic pain (*27*) and in other neurodegenerative and neuropsychiatric disorders (*28*). Glial cells display considerable diversity between and within distinct regions of the central nervous system (*29*). If the presently identified gliogenic LTP also existed at some brain areas, it could be of relevance not only for pain but also for other disorders, such as cognitive deficits, fear and stress disorders, and chronic immune-mediated diseases (*24*, *29*, *30*).

REFERENCES AND NOTES

1. T. V. P. Bliss, G. L. Collingridge, *Nature* **361**, 31–39 (1993).
2. H. Ikeda, B. Heinke, R. Ruscheweyh, J. Sandkühler, *Science* **299**, 1237–1240 (2003).
3. H. Ikeda *et al.*, *Science* **312**, 1659–1662 (2006).
4. R. Kuner, *Nat. Med.* **16**, 1258–1266 (2010).
5. X.-Y. Li *et al.*, *Science* **330**, 1400–1404 (2010).
6. R. Drdla, M. Gassner, E. Gingl, J. Sandkühler, *Science* **325**, 207–210 (2009).
7. R.-R. Ji, T. Berta, M. Nedergaard, *Pain* **154** (Suppl 1), S10–S28 (2013).
8. S. B. McMahon, M. Malcangio, *Neuron* **64**, 46–54 (2009).
9. P. M. Grace, M. R. Hutchinson, S. F. Maier, L. R. Watkins, *Nat. Rev. Immunol.* **14**, 217–231 (2014).
10. Q.-J. Gong *et al.*, *Glia* **57**, 583–591 (2009).
11. H. W. Tao, L. I. Zhang, F. Engert, M. Poo, *Neuron* **31**, 569–580 (2001).
12. A. K. Clark *et al.*, *J. Neurosci.* **35**, 4552–4570 (2015).
13. J. G. Gu, A. B. MacDermott, *Nature* **389**, 749–753 (1997).
14. Y.-X. Chu, Y. Zhang, Y.-Q. Zhang, Z.-Q. Zhao, *Brain Behav. Immun.* **24**, 1176–1189 (2010).
15. K. Kobayashi, E. Takahashi, Y. Miyagawa, H. Yamanaka, K. Noguchi, *Neurosci. Lett.* **504**, 57–61 (2011).
16. R. Aoyama *et al.*, *Pain* **152**, 2085–2097 (2011).
17. W.-J. He *et al.*, *Behav. Brain Res.* **226**, 163–170 (2012).
18. C. Ficker *et al.*, *Glia* **62**, 1671–1686 (2014).
19. J. Jung, Y. H. Shin, H. Konishi, S. J. Lee, H. Kiyama, *Biochem. Biophys. Res. Commun.* **430**, 488–493 (2013).
20. R. D. Fields, Y. Ni, *Sci. Signal.* **3**, ra73 (2010).
21. D. Gruber-Schoffnegger *et al.*, *J. Neurosci.* **33**, 6540–6551 (2013).
22. K. J. Sekiguchi *et al.*, *Nat. Commun.* **7**, 11450 (2016).
23. M. Martineau *et al.*, *J. Neurosci.* **33**, 3413–3423 (2013).
24. D. N. Xanthos, J. Sandkühler, *Nat. Rev. Neurosci.* **15**, 43–53 (2014).
25. R.-R. Ji, Z. Z. Xu, G. Strichartz, C. N. Serhan, *Trends Neurosci.* **34**, 599–609 (2011).
26. X.-H. Wei *et al.*, *J. Neurosci.* **33**, 1540–1551 (2013).
27. I. P. Chessell *et al.*, *Pain* **114**, 386–396 (2005).
28. A. M. Basso *et al.*, *Behav. Brain Res.* **198**, 83–90 (2009).
29. B. S. Khakh, M. V. Sofroniew, *Nat. Neurosci.* **18**, 942–952 (2015).
30. A. Aguzzi, B. A. Barres, M. L. Bennett, *Science* **339**, 156–161 (2013).

ACKNOWLEDGMENTS

This work was supported by grants P 29206-B27 and W1205 from the Austrian Science Fund (FWF) to J.S. We thank L. Czarnecki for laboratory support and B. Heinke and G. Janeselli for technical support. All of the data are archived on servers of the Center for Brain Research, Medical University of Vienna. The authors declare no conflicts of interest. M.T.K., R.D.-S., and J.S. designed the research. M.T.K., R.D.-S., M.G., S.D.H., and H.L.T. generated and analyzed the data. M.T.K., R.D.-S., and J.S. wrote the paper, with input from the other authors.

SUPPLEMENTARY MATERIALS

www.sciencemag.org/content/354/6316/1144/suppl/DC1
Materials and Methods
Figs. S1 to S6
Movie S1
References (*31*–*35*)

15 July 2016; accepted 1 November 2016
Published online 10 November 2016
10.1126/science.aah5715

STRUCTURAL BIOLOGY

Zika virus produces noncoding RNAs using a multi-pseudoknot structure that confounds a cellular exonuclease

Benjamin M. Akiyama,[1] Hannah M. Laurence,[1,2,3]* Aaron R. Massey,[4]* David A. Costantino,[1] Xuping Xie,[5] Yujiao Yang,[5] Pei-Yong Shi,[5] Jay C. Nix,[6] J. David Beckham,[4] Jeffrey S. Kieft[1,7]†

The outbreak of Zika virus (ZIKV) and associated fetal microcephaly mandates efforts to understand the molecular processes of infection. Related flaviviruses produce noncoding subgenomic flaviviral RNAs (sfRNAs) that are linked to pathogenicity in fetal mice. These viruses make sfRNAs by co-opting a cellular exonuclease via structured RNAs called xrRNAs. We found that ZIKV-infected monkey and human epithelial cells, mouse neurons, and mosquito cells produce sfRNAs. The RNA structure that is responsible for ZIKV sfRNA production forms a complex fold that is likely found in many pathogenic flaviviruses. Mutations that disrupt the structure affect exonuclease resistance in vitro and sfRNA formation during infection. The complete ZIKV xrRNA structure clarifies the mechanism of exonuclease resistance and identifies features that may modulate function in diverse flaviviruses.

Globalization, urbanization, and climate change contribute to the spread of pathogenic mosquito-borne viruses, typified by the outbreak of Zika virus (ZIKV) (*1*). ZIKV infection can cause fetal microcephaly and Guillain-Barré syndrome (*2*), motivating efforts to understand the molecular drivers of pathology. ZIKV is a (+)-sense single-stranded RNA mosquito-borne flavivirus (MbFV) related to dengue virus (DENV), yellow fever virus (YFV), and West Nile virus (WNV) (*3*). The structured 3′ untranslated regions (UTRs) of many MbFVs are the source of noncoding subgenomic flaviviral RNAs (sfRNAs) that accumulate during infection when RNA elements resist degradation by the host 5′ → 3′ exonuclease Xrn1 (fig. S1A) (*4*). These sfRNAs are directly linked to cytopathic and pathologic effects (*4*); they dysregulate RNA decay pathways and bind cellular proteins important for antiviral responses (*5*–*14*). Preventing sfRNA production could be a strategy for targeted therapeutics or for generating attenuated virus for vaccines (*15*–*17*).

Because sfRNA formation during ZIKV infection has not been reported, we infected multiple cell lines with ZIKV strain PRVABC59, isolated in 2015 from an infected U.S. mainland–Puerto Rico traveler. Northern blot analysis of total RNA isolated from infected cells showed discrete bands containing parts of the ZIKV 3′UTR, consistent with sfRNAs (Fig. 1A). Mouse primary neuron infection resulted in very little infectious virus and produced three weak sfRNA bands. Infection of C6/36 (*Aedes albopictus* mosquito) cells produced two predominant sfRNAs, whereas Vero (monkey) and A549 (human) epithelial cell infection produced additional bands. Different cell types produced different sfRNA patterns, but the largest sfRNA was present in all. The importance of this cell type–dependent variation in the sfRNA patterns is unknown, although studies with DENV suggest that sfRNA production is modulated to enable host adaptation (*16*, *18*).

The production of ZIKV sfRNAs suggests the existence of Xrn1-resistant structures (xrRNAs) in the viral 3′UTR. Two areas of the UTR match the sequence pattern and potential secondary structure of known MbFV xrRNAs (Fig. 1, B and C, and fig. S1B) (*4*, *18*). The putative xrRNAs are in series near the 5′ end of the UTR—a location and pattern similar to that of other MbFVs (Fig. 1D). Xrn1 halting at putative ZIKV xrRNA1 and xrRNA2 would result in sfRNAs of sizes matching the two produced in all cell types tested (Fig. 1A and fig. S1C). To test whether these putative elements are indeed Xrn1-resistant, we challenged in vitro transcribed full-length ZIKV 3′UTR RNA with recombinant Xrn1 (*19*). Although multiple sfRNAs were observed during ZIKV infection, in vitro the upstream xrRNA1 quantitatively halted the enzyme (Fig. 1E). However, a UTR lacking the upstream xrRNA (ΔxrRNA1) allowed the enzyme to stop at the downstream xrRNA2. The size of the Xrn1-resistant RNAs matched those of the infection-produced sfRNAs (fig. S1D). Thus, ZIKV

[1]Department of Biochemistry and Molecular Genetics, University of Colorado Denver School of Medicine, Aurora, CO 80045, USA. [2]Howard Hughes Medical Institute (HHMI), University of Colorado Denver School of Medicine, Aurora, CO 80045, USA. [3]School of Veterinary Medicine, University of California, Davis, CA 95616, USA. [4]Department of Medicine, Division of Infectious Diseases, University of Colorado Denver School of Medicine, Aurora, CO 80045, USA. [5]Department of Biochemistry and Molecular Biology, University of Texas Medical Branch, Galveston, TX 77555, USA. [6]Molecular Biology Consortium, Advanced Light Source, Lawrence Berkeley National Laboratory, Berkeley, CA 94720, USA. [7]RNA BioScience Initiative, University of Colorado Denver School of Medicine, Aurora, CO 80045, USA.
*These authors contributed equally to this work. †Corresponding author. Email: jeffrey.kieft@ucdenver.edu

Gliogenic LTP spreads widely in nociceptive pathways
M. T. Kronschläger, R. Drdla-Schutting, M. Gassner, S. D. Honsek, H. L. Teuchmann and J. Sandkühler (November 10, 2016)
Science **354** (6316), 1144-1148. [doi: 10.1126/science.aah5715]
originally published online November 10, 2016

Editor's Summary

Glial cells contribute to pain

Pain hypersensitivity can spread to unaffected body regions immediately surrounding the initial insult. Sometimes it can even spread to the opposite site of the body or to large body areas and cause widespread pain. Kronschläger *et al.* discovered a form of synaptic plasticity in the spinal cord that may explain the spread of pain hypersensitivity. This plasticity was induced by the activation of glial cells. The spread was mediated by gliotransmitters that diffuse widely, even reaching the cerebrospinal fluid at biologically relevant concentrations.

Science, this issue p. 1144